THE STRENGTH OF THE
SUN'S POLAR FIELDS

By

Leif Svalgaard

Thomas L. Duvall, Jr.

Philip H. Scherrer

D D C

RECEIVED

MAY 11 1978

F

SUIPR Report No. 737

January 1978

INSTITUTE FOR PLASMA RESEARCH
STANFORD UNIVERSITY, STANFORD, CALIFORNIA

SECURITY CLASSIFICATION OF THIS PAGE (When Data Entered)

REPORT DOCUMENTATION PAGE		READ INSTRUCTIONS BEFORE COMPLETING FORM
1. REPORT NUMBER SUIPR Report No. 737	2. GOVT ACCESSION NO. SU-IPR-737	3. RECIPIENT'S CATALOG NUMBER
4. TITLE (and Subtitle) THE STRENGTH OF THE SUN'S POLAR FIELDS		5. TYPE OF REPORT & PERIOD COVERED Scientific, Technical
		Scientific repts
		6. PERFORMING ORG. REPORT NUMBER
7. AUTHOR(s) L. Svalgaard, T.L. Duvall, Jr., P. Scherrer		8. CONTRACT OR GRANT NUMBER(s) N00014-76-C-0207, NGR-05-020-559
9. PERFORMING ORGANIZATION NAME AND ADDRESS Institute for Plasma Research Stanford University Stanford, California 94305		10. PROGRAM ELEMENT, PROJECT, TASK AREA & WORK UNIT NUMBERS
11. CONTROLLING OFFICE NAME AND ADDRESS Office of Naval Research Electronics Program Office Arlington, Virginia 22217		12. REPORT DATE January 1978
		13. NO. OF PAGES 20
14. MONITORING AGENCY NAME & ADDRESS (if diff. from Controlling Office)		15. SECURITY CLASS. (of this report) Unclassified
		15a. DECLASSIFICATION/DOWNGRADING SCHEDULE

16. DISTRIBUTION STATEMENT (of this report)

This document has been approved for public release and sale;
its distribution is unlimited.

17. DISTRIBUTION STATEMENT (of the abstract entered in Block 20, if different from report)

18. SUPPLEMENTARY NOTES

Tech; other

19. KEY WORDS (Continue on reverse side if necessary and identify by block number)

magnetic field strength
solar/polar fields

20. ABSTRACT (Continue on reverse side if necessary and identify by block number)

332,630

THE STRENGTH OF THE SUN'S POLAR FIELDS

By

Leif Svalgaard
Thomas L. Duvall, Jr.
Philip Scherrer

SUIPR Report No.   737

January 1978

Institute for Plasma Research
Stanford University
Stanford, California

Submitted to: Solar Physics

THE STRENGTH OF THE SUN'S POLAR FIELDS

by

Leif Svalgaard, Thomas L. Duvall, Jr.
and Philip H. Scherrer
Institute for Plasma Research
Stanford University
Stanford, California 94305

Introduction

The magnetic field strength within the polar caps of the sun is
an important parameter for both the solar activity cycle and for our
understanding of the interplanetary magnetic field. Measurements of
the line-of-sight component of the magnetic field generally yield
0.1 to 0.2 mT (e.g., Severny, 1971; Howard, 1974a) near times of sun-
spot minimum. Near sunspot maximum the field weakens and reverses
polarity (Babcock, 1959; Howard, 1974a). At the present solar minimum,
magnetic field strengths at latitudes above 60° are observed to be in
the 0.0 to 0.2 mT range. In a recent study, Howard (1977) concludes
that the "true" field strength is unlikely to be more than twice the
measured values, and that it is impossible that it could be greater
than the measured line-of-sight values by more than a factor of five.

The true magnetic field strength is not the same as the average
field strength measured by the solar magnetograph because the bulk
of the magnetic flux is confined to sub-arc second bundles of field
lines where field strengths are of the order of 100-200 mT (Stenflo, 1973).
It would be more correct to acknowledge this fact by referring to an
average flux density over some area on the sun rather than to a field
strength.

In this paper we report measurements of the polar fields made at
the Stanford Solar Observatory using the FeI line $\lambda525.02$ nm
(Scherrer et al., 1977; Duvall, 1977). We find that the average
flux density poleward of 55° latitude is about 0.6 mT peaking to
more than 1 mT at the pole and decreasing to 0.2 mT at the polar
cap boundary. The total open flux through either polar cap thus

becomes about 3×10^{14} weber.

Observational details

In the magnetograph mode the solar image is scanned with a
175" x 175" square aperture. The image is divided into 11 scan
lines (Figure 1) parallel to the solar equator The aperture is
stepped one-half aperture between each measurement. A typical
error for both the magnetic signal and the zero level is 5 μT.
Figure 2 shows a typical magnetogram. Three active regions all
belonging to the new sunspot cycle - number 21 - are clearly seen.
In addition, extensive background fields are apparent including well-
defined polar fields. Referring to Figure 1 we shall be particularly
interested in the field measured in the polar cap, i.e. the polemost
scan line in each hemisphere. The average latitude of the equator-
ward limit of that aperture is 55°. At the present time that is also
the equatorward boundary of the polar coronal holes (Solar Geophysical
Data, 1976, 1977). In accordance with that, the measured polar fields
have invariably been unipolar (over the aperture) throughout the
interval covered by the daily magnetograms - 16 May 1976 through
August 1977 - positive or outwards in the north and negative or in-
wards in the southern polar cap. The position of an aperture along
the scan line is measured by the parameter x, being 0 at central
meridian, and $\pm$11 respectively at the west - and east equatorial
limbs (Figure 1). We shall be concerned with apertures at x = 0
(black in Figure 1) and at x = $\pm$2 (dotted areas in Figure 1).
During the course of a year the solar rotation axis tips toward and
later away from the observer by $7\frac{1}{4}^{\circ}$. We thus get a kind of stereo-
scopic view of the polar fields provided that they do not change
appreciably over a timescale of up to a year.

In order to interpret measurements of the polar cap fields, it is
necessary to investigate if the fact that the data is taken near the
limb is distorting the data in any way. It has been suggested by
Howard and Stenflo (1972) that measurements of the magnetic field in
the λ525.02 nm line are systematically in error by a factor that

2

depends on the angle between the radius and the line of sight.
This error changes by more than a factor of two as one goes from the
center of the disk to the limb. By following specific areas as they
cross the disk from east limb to west limb in the course of solar
rotation we may directly verify the existence of this systematic
error under the weak assumption that the intrinsic field does not
change considerably during disk passage. In the following section
we report the results of an extensive analysis of measured field
strengths as a function of the distance from disk center. Our con-
clusion is that no systematic error of the kind suggested by Howard and
Stenflo (1972) is apparent in the Stanford data.

Center to limb variation of field strength

When an aperture is placed at central meridian an area is defined
on the solar surface. The area can be assigned heliographic coordinates
and can be identified on magnetograms both before and after central
meridian passage. For the analysis we utilize the three near-
equatorial scan lines - ranging up to 16° in latitude on either side
of the equator. If the dominent effect that determines the line-of-
sight component, B_{ℓ}, of the field B is simple projection, the observed
longitudinal field should vary as $B_{\ell} = B \cos L$ where L is the angle be-
tween the radius vector and the line of sight (Figure 3). Figure 4
shows the average B_{ℓ} as a function of cosL. The analysis was performed
separately for weak fields ($|B| < 150 \, \mu T$) and for strong fields
($|B| \geq 150 \, \mu T$). The magnetic field strength at central meridian passage
was used as the selection parameter. Furthermore, the data was analyzed
separately for each polarity of the field. More than 90% of the data
fall in the weak field category - which ultimately also includes the
polar regions. It is difficult to assess the error bars in Figure 4
because the data is not independent but conservative estimates based
on the standard deviation of the values going into each average point
lead to standard errors of the mean of $\pm 1 \, \mu T$ for the weak field case
and of $\pm 50 \, \mu T$ for the strong field case. It appears that the observed
field strength is very nearly proportional to cosL. There is a small
asymmetry between east and west hemispheres: at the east limb a small

3

net negative field is observed, while at the west limb a net positive field is seen. The imbalance is caused by a weak net azimuthal field first observed by Howard (1974b) and discussed in detail by Duvall (1977). Folding the west hemisphere onto the east hemisphere data eliminates this azimuthal field component as shown by the lower line in Figure 5. Also shown in Figure 5 is the result of a similar analysis of the latitude band $16^{\circ}-32^{\circ}$. In this latitude band most of the active regions have appeared over the time interval covered by the analysis. The aperture at disk center corresponds to a certain area on the solar surface ($1.7 \times 10^{10} km^2$); at some distance from disk center the area is larger. This increases the chances that more active region flux cancels inside the aperture and thus lowers the observed average field strength. This effect can be discerned in Figure 5 for the $16^{\circ}- 32^{\circ}$ latitude bands for small values of cos L - corresponding to a larger area within the aperture.

The overall result seems to be that the measured magnetic field values fall off very nearly as cos L from central meridian to the limb, i.e., consistent with the interpretation of the observed field being just the line-of-sight component of the real field By assuming that the field measured using FeI $\lambda523.3$ nm represents the true average field - unaffected by Zeeman saturation and line weakening - Howard and Stenflo (1972) suggested that the field as observed in $\lambda525.0$ nm should be corrected by a factor $(0.48 + 1.33 \cos \rho)^{-1}$ where ρ is the angle between line-of-sight and the radius vector. In Figure 6 we show the center-to-limb variation of a radial field of 51 μT as it would be observed at Stanford and as it should be observed if the correction factor suggested by Howard and Stenflo (1972) is applied. The linear dependence on cos L shown by the Stanford data (Figure 4) is clearly inconsistent with any such correction. The reason for this discrepancy is not known, but collaborative work is in progress to clear up the matter. One might speculate (Stenflo, personal communication 1977) that since the field observed in the $\lambda523.3$ nm line does not refer to the same height in the photosphere at the center of the disk and at the limb, a rapid divergence of the field lines in the upper photosphere where the

4

λ523.3 nm line is formed may distort the center-to-limb variation of the measured fields. In the deeper layers where λ525.0 nm is formed the divergence is probably insignificant. The verification of this requires detailed calculations with fluxtube models and multi-dimensional radiative transfer and is outside the scope of the present paper. At the present time, we adopt the simplest interpretation, namely that the low-noise Stanford magnetograms indicate that magnetic field strength values obtained in the λ525.0 nm line can be corrected for foreshortening by dividing with cosine of the angle between the radius vector and the line-of-sight.

These considerations have implications for the computation of potential magnetic fields in the corona. In the past Mt. Wilson λ525.0 nm data has been used with the correction suggested by Howard and Stenflo (1972), e.g. Riesebieter (1977), and Kitt Peak λ523.3 nm data have been used assuming no distortion of the limb data due to field line divergence, e.g. Altschuler et al.,(1977). Quantitative results from these calculations, e.g. Levine et al.,(1977), should now be considered suspect.

Magnetograph saturation

At Stanford we use the same slit sizes and arrangement as at Mt. Wilson for the line λ525.02 nm. The two exit slits are λ7.5 pm wide and have a separation of λl.8 pm. With these slits the magnetic signal as a function of effective Zeeman splitting is shown in Fig. 7. The curve in Fig. 7 is obtained by placing a right-hand circular polarizer in front of the KDP crystal and recording the magnetic signal while scanning across the line. For weak fields (i.e., less than 50 mT) the magnetic signal is proportional to the field strength. As the field increases the magnetograph response weakens and at 143 mT the magnetograph is saturated and any further increase of the field actually decreases the magnetic signal. Assuming that a typical field strength within the magnetic elements is 150 mT (Stenflo, 1973; Ramsey, et al., 1977) the corresponding reading from the magnetograph would be only 83 mT; hence the effect of magnetograph saturation due to the strong fields in the elements is to reduce the measured flux by a factor $150/83 = 1.8$.

The careful, lengthy analysis by Stenflo (1973) gives essentially the same result. If the polar fields also exist mainly in the form of elements of the same strength as in lower latitudes we might expect a similar reduction of the measured flux. No detailed study of this problem has been carried yet specifically within the polar caps but preliminary data from the Stanford Solar Observatory suggests that there is no difference in the saturation between the polar and the equatorial limbs.

Polar field strengths

In order to set the stage for the discussion of the Stanford data, Fig. 8 shows the average line-of-sight magnetic field strength poleward of 69° latitude (filled symbols) and between 60° and 69° (open symbols) observed at Mt. Wilson since 1971 following the polar field reversal around 1970. Average field strengths polewards of 55° as observed at Stanford during 1976 and 1977 appear as symbols with crosses and seem to concur with the Mt. Wilson averages. Assuming that the polar fields are radial and that an effective latitude of the polar cap is 70° we may arrive at a first crude estimate of the true field strength.

$$B_{true} = (\pm\ 100\ \mu T/\cos\ 70^{\circ}) \times 1.8 = 0.5\ mT$$

The Stanford data allows us to extend the analysis considerably. If the polar fields were indeed uniform and radial they would not change during the year as the rotation axis tips back and forth by $7\frac{1}{4}^{\circ}$. Figure 9 shows that the polar fields change by about a factor of two during the year. We have plotted monthly averages of the field strengths through polar scan line apertures $x = 0$ and $x = \pm\ 2$ for both hemispheres. There can be no doubt about the reality of the apparent yearly variation shown in Fig. 9. The uncertainty in each average point is less than $10\ \mu T$ and is mainly due to solar causes rather than instrumental errors. Times of maximum tilt away from the observer are indicated by arrows while times of maximum tilt towards the observer are marked by short vertical lines.

6

To proceed we now introduce a model of the polar field geometry.
Judging from the inclination of polar plumes in eclipse photographs,
it seems likely that the magnetic field lines at high latitudes are
inclined toward the equator. We therefore introduce a meridional field
component, B_θ, arising from a field inclination α against the radial,
(Figure 10). The radial component is modeled by the expression

$$B_r = B_p \cos^n \theta$$

and also

$$B_\theta = B_r \tan \alpha$$

where

$$\alpha = q\theta \qquad .$$

Here n and q are the two parameters of the model with B_p providing
the calibration being the field strength at the very pole. n = 0 is
the case of a uniform radial component of the field across the polar
cap, while a large value of n indicates a field distribution highly
peaked towards the pole. Similarly q = 0 corresponds to a purely
radial field, while q $\simeq$ 1 is typical of the inclination of the polar
plumes. A dipole field has q $\simeq$ 0.5 within the polar cap. By varying
n and q a wide range of field geometries can be accommodated.

The next step is to calculate the average line-of-sight component
of the model field properly weighted by limb darkening within each of
our apertures for various values of polar axis tilt angle. Of special
interest are the two cases of maximum tilt away from and towards the
observer. In the model calculations B_p is set equal to one. Let the
computed average be $<B>_{comp}$ and the observed value be B_{obs}, then
$B_p = B_{obs}/<B>_{comp}$ is our calibration constant. The ratio between
the average model fields through a given aperture for the pole tipped
toward us and for the pole tipped away from us by the maximum amount,
i.e.

$$r = \frac{<B>_{comp} \,[\text{toward}]}{<B>_{comp} \,[\text{away}]}$$

is a simple measure of the non-uniformity of the magnetic fields within

the polar cap. This ratio was observed to be about 2[*]. Figure 11 shows the computed ratio as a function of n and q. The solid contours are for the aperture x = 0, while dashed contours are for the case x = ± 2. It is fortunate that the contours for the two cases do not run nearly parallel to each other. As things stand it seems possible to conclude that n = 8 ± 1 and q = 0.0 ± 0.1 fits the observed value of r = 2.1 uniquely. The resulting B_p turns out to be 0.64 mT. The variation of B with latitude is shown in Fig. 12. The ordinate scale on the left is for field strengths observable with λ525.02. On the right the effect of magnetograph saturation is incorporated by scaling with the factor 1.8. We see that the data is consistent with rather high field strengths at the pole ($B_p = 1.15$ mT) falling rapidly off with colatitude until about 0.2 mT at the polar cap boundary. It is essentially this strong peaking of the field strength near the pole that causes the large change of line-of-sight field with time of year as seen in Fig. 9.

The polar cap magnetic flux is given by

$$F = R_\odot^2 \int_0^{\theta_c} \int_0^{2\pi} B(\theta) \sin \theta \, d\lambda \, d\theta = 2\pi \, R_\odot^2 \, B_p \, \frac{1}{9} \, (1 - \cos^9 \theta_c)$$

where θ_c is the colatitude of the polar cap boundary. Because the area of the polar cap is $A = 2\pi \, R_\odot^2 \, (1 - \cos \theta_c)$ the average field strength becomes

$$< B >_{cap} = B_p \cdot \frac{1}{9} \, \frac{1 - \cos^9 \theta_c}{1 - \cos \theta_c} = 0.51 \, B_p$$

$$= 0.65 \text{ mT} \quad .$$

It is worth pointing out that the polar cap flux, $F = 3.24 \times 10^{14}$ Wb, is almost sufficient to provide the interplanetary magnetic flux ($F_{IMF} = 5 \times 10^{14}$ Wb for each hemisphere). With additional flux entering the solar wind from low latitude magnetic sectors it seems that the interplanetary magnetic flux is easily accounted for at least when

---

[*] A more detailed analysis gives r = 2.1 ± 0.1 for both apertures shown in Fig. 9.

8

the polar fields are strong near sunspot minimum. At times shortly after sunspot maximum the equatorial sectors must supply all the necessary flux to maintain the observed constancy of the interplanetary magnetic field (e.g. King, 1976).

Coronal holes

It is often assumed (e.g., Hundhausen, 1977; Levine, 1977; Suess et al., 1977) that coronal holes have unique properties independent of their position on the sun; in particular that the photospheric magnetic field strength is always the same within coronal holes, namely about 1 mT. During the interval of our observations (May 1976 - August 1977) there were only a few and ill-defined equatorial holes (Solar Geophysical Data, 1976, 1977). The polar caps had however prominent extensions or lobes towards lower latitudes. These extensions are long lived and occur near the middle of magnetic sectors (e.g., Wilcox and Svalgaard, 1974). A particularly good example can be found in the northern hemisphere around heliographic longitude 275° during Carrington rotation 1651 - 1653. The magnetic field within the hole was rather constant and is shown in Fig. 12 as open circles. It appears that this coronal hole magnetically can be described as an extension of the polar cap; the field strength of 0.15 mT being typical of polar cap boundary conditions. It would seem that physical models of coronal holes would benefit from the more realistic estimates of the magnetic field strength suggested in the present paper.

In a numerical simulation of conditions within the northern polar hole during July 1973 from $2R_{\odot}$ to $5 R_{\odot}$, Suess et al. (1977) show that the dominant source of divergence within $5 R_{\odot}$ is the meridional gradient of the magnetic field strength. The resulting meridional magnetic pressure gradient relieves itself through meridional plasma flow producing the observed large spreading of the polar hole with altitude. The magnetic field geometry deduced in the present paper is entirely consistent with these ideas.

9

Summary

   Observations at Stanford Solar Observatory of solar magnetic fields
in the FeI line $\lambda525.02$ nm shows that a radial magnetic field measured
at a point where the radius makes an angle ρ with the line of sight
is observed to be decreased by a factor cos ρ. For field elements of
150 mT, magnetograph saturation causes the measured field to be too
low by a factor of 1.8. The average field magnitude poleward of 55°
latitude is measured to be near 100 μT. Variation of the apparent field
over a 3 arc min aperture grazing the limb at central meridian amounts
to a factor of two over the year; the field being strongest when the
pole is tipped the most $(7\frac{1}{4}^{o})$ towards the observer. Combination of all
the above results leads to the following picture of the magnetic field
within the polar caps. The field is nearly radial, varying as $B_p \cos^8 \theta$
where the field strength B_p at the pole $(\theta = 0^{o})$ is 1.15 mT, and fall-
ing off to below 0.2 mT at the polar cap boundary $(\theta = 35^{o})$. Within
coronal holes outside of the polar cap the magnetic field strength at
sunspot minimum is rather small (0.15 mT). At other phases of the sun-
spot cycle the relative strengths of polar and lower latitude field
magnitudes is very likely different from what is observed at the present
sunspot minimum.

REFERENCES

Altschuler, M.D., Levine, R.H. Stix, M., and Harvey, J., 1977, Solar
Phys., 51, 345.

Babcock, H.D., 1959, Ap. J., 130, 364.

Duvall, T.L., Jr., 1977, Ph.D. Thesis, Stanford University, Dept. of
Applied Physics.

Howard, R., 1974a, Solar Phys., 38, 283.

Howard, R., 1974b, Solar Phys., 39, 275.

Howard, R., 1977, Solar Phys., 52, 243.

Howard, R. and Stenflo, J.O., 1972, Solar Phys., 22, 402.

Hundhausen, A.J., 1977, in Coronal Holes., ed., J. Zirker, Colorado
Associated University Press, Boulder.

King, J.H., 1976, J. Geophys. Res., 81, 653.

Levine, R.H., Altschuler, M.D., Harvey J.W., and Jackson, B., 1977,
Ap. J., 215, 636.

Ramse, H.E., Schoolman, S.A., and Title, A.M., 1977, Ap. J. (Letters),
215, L41.

Riesebieter, W., 1977, Dissertation, Nat. Fakultat der Tech. Univ.
Carolo-Wilhelmina zu Braunschweig.

Scherrer, P.H., Wilcox, J.M., Svalgaard, L., Duvall, T.L., Jr.,
Dittmer, P.H., and Gustafson, E.K., 1977, Solar Phys., (in press).

Severny, A.B., 1971, IAU Symp. 43, 675.

Solar Geophysical Data 1976, U.S. Dept. of Commerce.

Solar Geophysical Data 1977, U.S. Dept. of Commerce.

Stenflo, J.O., 1973, Solar Phys., 32, 41.

Suess, S.T., Richter, A.K., Winge, C.R., and Nerney, S.F., 1977,
Ap. J., 217, 296.

Wilcox, J.M. and Svalgaard, L., 1974, Solar Phys., 34, 461.

FIGURE CAPTIONS

Fig. 1.   Scan lines across the solar disk. The poleward scans begin at
          latitude 55° if the poles are in the plane of the sky. The
          aperture is shown in the lower right. Marked in black are the
          polar, central meridian apertures ($x = 0$). Marked as dotted
          areas are further apertures ($x = \pm 2$) used in the analysis.

Fig. 2.   Typical Stanford magnetogram (March 5, 1977). Solid contours
          denote positive fields while dashed contours denote negative
          fields. Three active regions are readily seen as well as ex-
          tended areas of background fields. Contour levels are ± 0.02,
          ± 0.05, ± 0.1, ± 0.2, ± 0.5, ± 1, ± 2 mT.

Fig. 3.   Definition of the angle L and line-of-sight component B_{ℓ} for a
          radial field in the equatorial plane.

Fig. 4.   Upper panel: Observed center-to-limb variation of measured
          magnetic field B_{ℓ} for weak average fields (less than 150 μT
          at central meridian). Data within 16° of the equator is used.
          Open symbols signify positive fields and filled symbols show
          the variation of negative fields. Each point is an average of
          more than 500 measurements.
          Lower panel: Same as above, but for strong fields only (greater
          than or equal to 150 μT at central meridian passage). The number
          of cases is much lower than for the weak field regions and the
          scatter is correspondingly larger. In addition, the assumption
          of constant intrinsic field strength for the two-week disk
          passage is more likely to be invalid for these strong fields.

Fig. 5.   Folding east-hemisphere data onto west-hemisphere data and
          negative field magnitudes onto positive field magnitudes results
          in a single curve showing field magnitude as a function of cos L
          from central meridian ($L = 0^{\circ}$) to the limb ($L = 90^{\circ}$). The
          filled circles show the result for the weak field case of Fig. 4.
          Open circles show the result of a similar analysis for the lati-
          tude bands (16°-32° in both hemispheres. Here all fields were
          included and the effect of flux cancellation within apertures
          closer to the limb can be discerned. The straight lines were

forced to go through zero at the limb. The main result of
Figs. 4 and 5 is that we are simply measuring longitudinal
magnetic fields.

Fig. 6.   Filled circles show how a magnetic field of 51 μT at central
meridian would be observed at Stanford (B_s) to change towards
the limb as a function of cos L. Assuming that B_s is the true
average longitudinal field, the field (B_w) that would be
observed at Mount Wilson as obtained by applying the Howard
and Stenflo (1972) correction is shown with open circles.
Normalizing the B_w curve to give the same field at disk center
as observed at Stanford yields the dotted curve (crosses).
It is clear that the Stanford data (Fig. 5) is inconsistent
with any systematic error of the kind proposed by Howard and
Stenflo.

Fig. 7.   Calibration curve for the Stanford magnetograph for the FeI
line λ525.02 nm and for exit slits λ7.5 pm wide separated by
λ1.8 pm. A magnetic field B produces a Zeeman splitting of
$\Delta\lambda = 38.6$ B pm/T. This relation is shown as the dotted line
and is also used to calibrate the scale along the upper right
boundary of the figure frame. Slit dimensions are shown in
the middle of the figure.

Fig. 8.   Yearly means of polar field strengths observed at Mt. Wilson
(open and filled symbols) and at Stanford (symbols with crosses)
since the polar field reversals in cycle 20. For Mt. Wilson
the average fields poleward of 69° (filled symbols) and between
60° and 69° latitude (open symbols) are shown separately for a
strip 10° wide in longitude and centered on central meridian.
For Stanford the average field through the x = 0 aperture of
the polemost scan line is plotted. For a uniform field the
average line-of-sight field polewards of 69° should be only 40%
of the line-of-sight field between 60° and 69°. We see here
the first hint of a considerable flux concentration towards
the pole.

Fig. 9. Yearly variation of magnetic field strength averaged over pole-
         ward apertures x = 0 (upper panel) and x = ± 2 (lower panel)
         observed at Stanford May 1976 - August 1977. Times of maximum
         heliographic latitude of the earth are marked by vertical
         lines and arrows. Open circles represent data from May-
         August 1976 that are plotted as May - August one year later. Each
         data point is a monthly average.

Fig. 10. Definition of the field inclination α and relations between
         radial, meridional and line-of-sight components.

Fig. 11. Contour plots of ratio between computed average line-of-sight
         magnetic field through poleward apertures x = 0 (solid lines)
         and x = ± 2 (dashed lines) for maximum tilt of the rotation
         axis towards and away from the observer. This ratio is computed
         in (n, q) space, i.e., as a function of the tendency for the
         magnetic flux to concentrate at the pole (increasing n) and as
         a function of inclination of the field towards the radial
         (increasing q).

Fig. 12. Variation with latitude of the inferred average magnetic flux
         density between the pole and the polar cap boundary. The
         ordinate scale on the right reflects the effect of correcting
         for magnetograph saturation by multiplying the measured flux
         density by 1.8. Open circles show the magnetic flux density
         for a coronal hole at 40° - 60° N and near 275° Carrington
         longitude. This hole was prominent during Carrington rotations
         1651-1653.

18

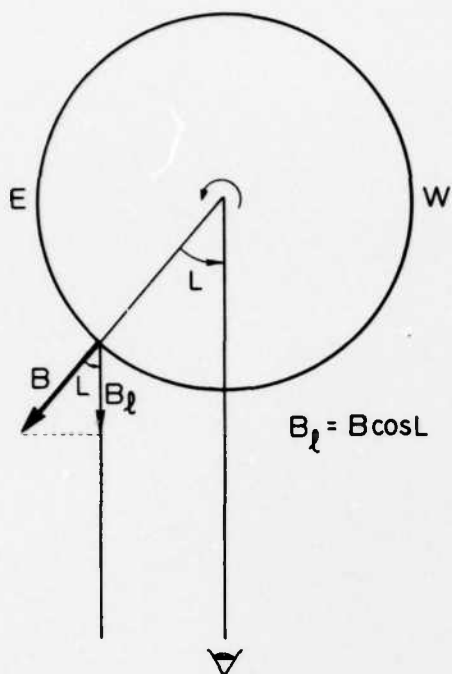Figure 1

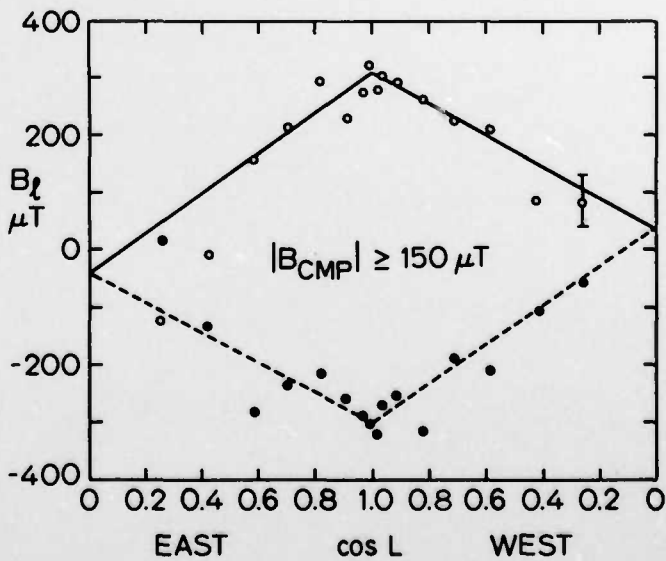
Figure 2

Figure 3

Figure 4

16

CENTER   LIMB

16°-32°

ALL FIELDS

0°-16°

WEAK FIELDS

Figure 5

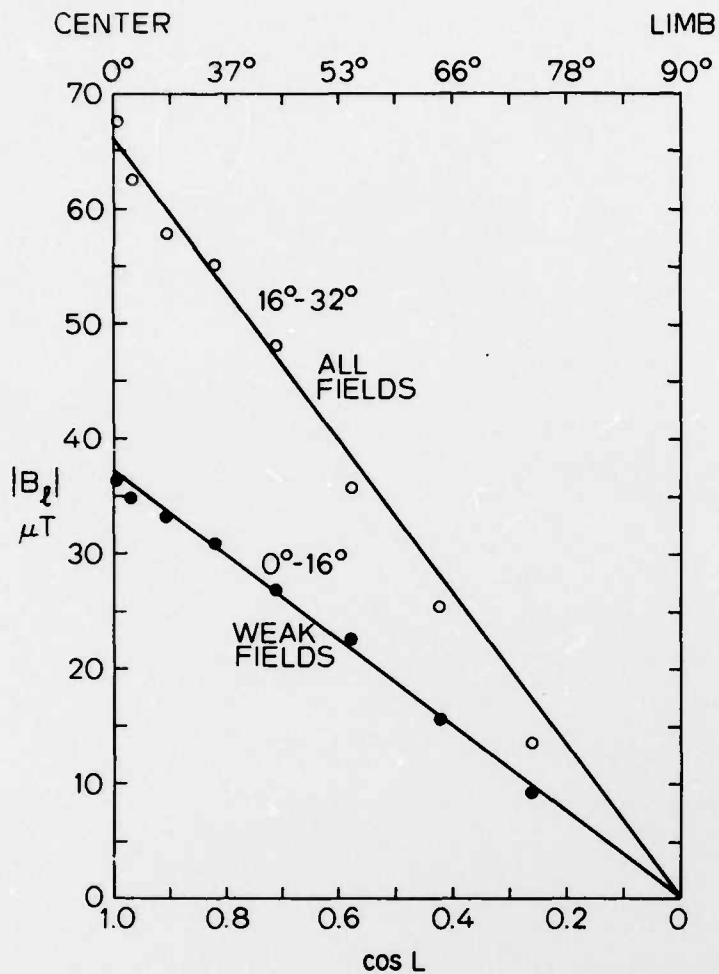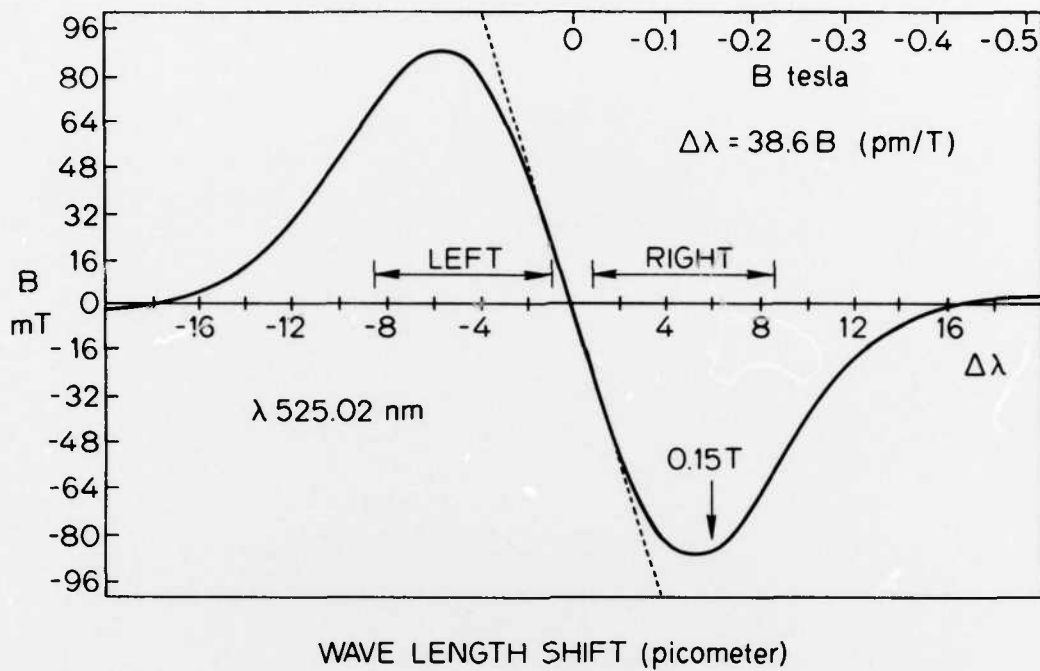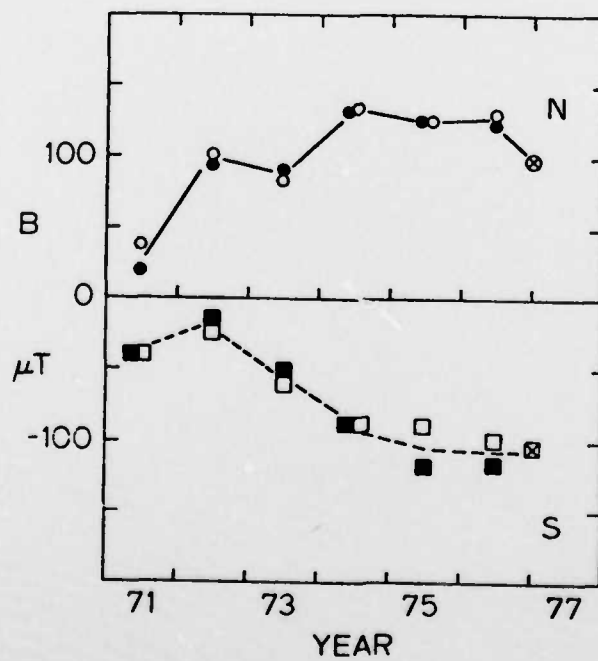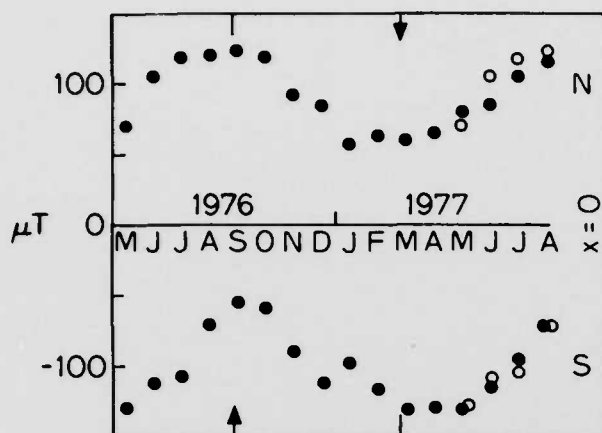Figure 6

$B_S = 51 \cos L \ \mu T$
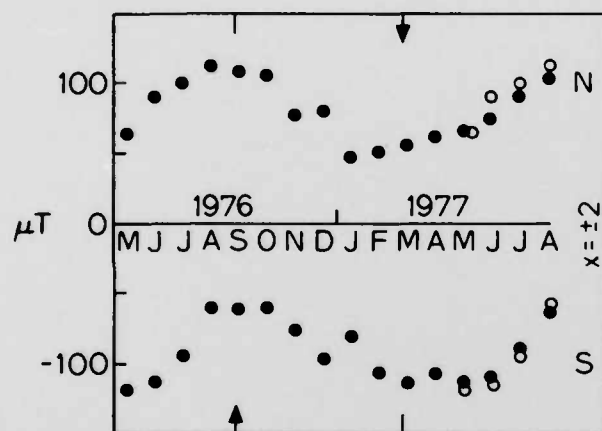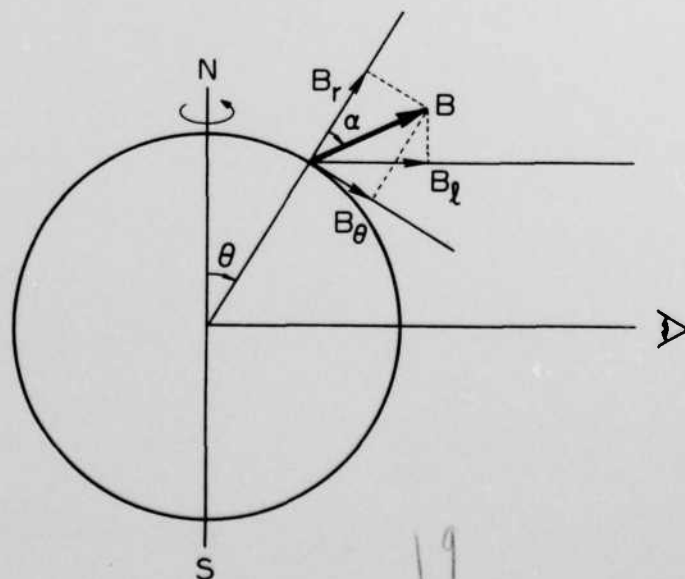
B_W norm.

$B_W = B_S (0.48 + 1.33 \cos L)^{-1}$
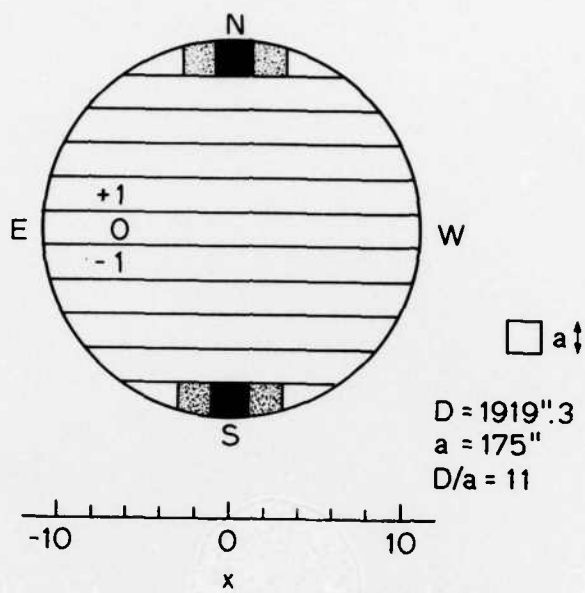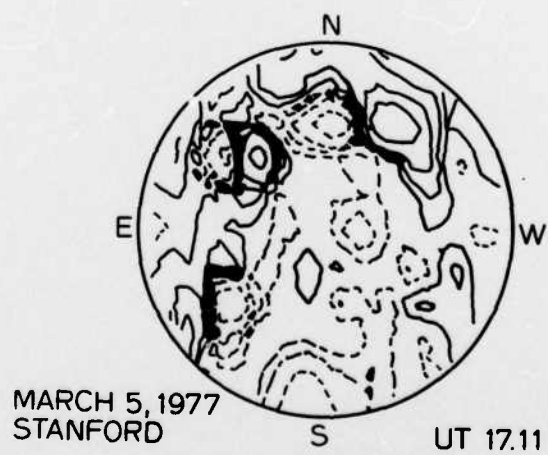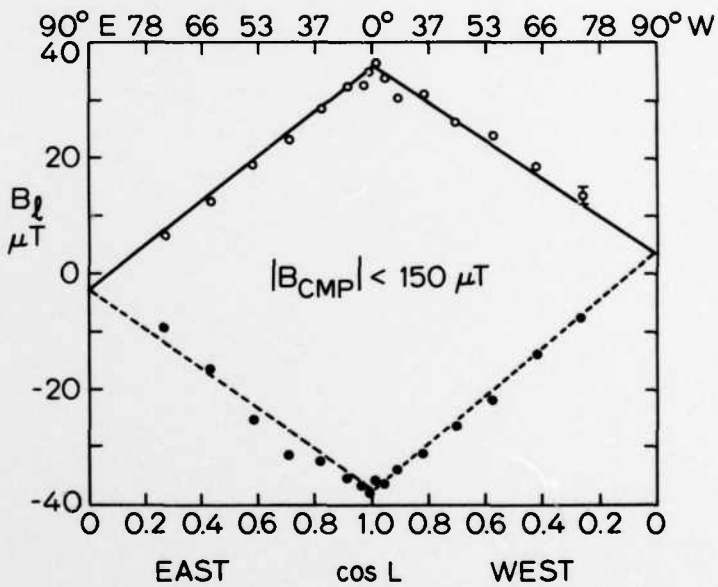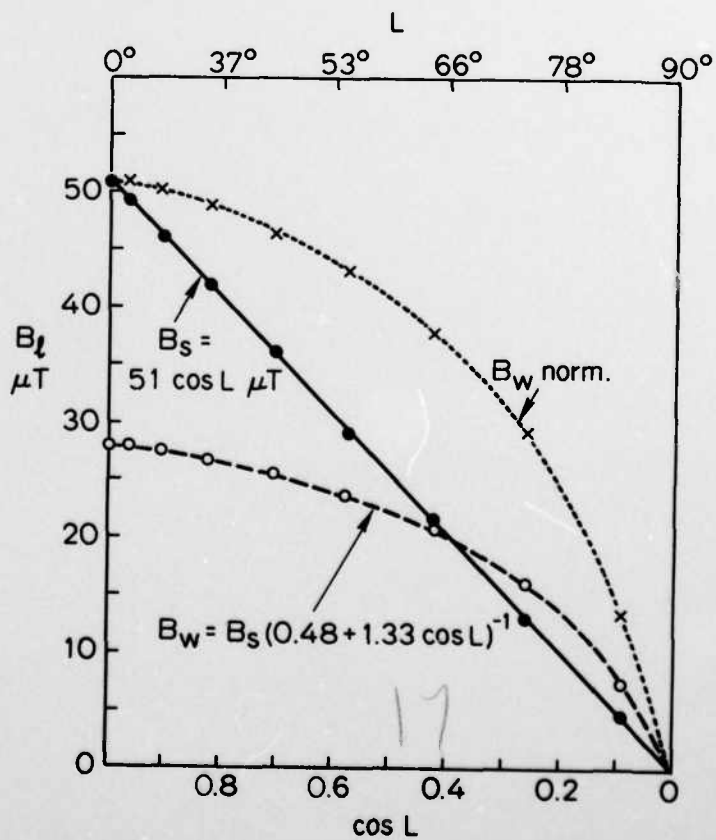
Figure 7

Figure 8

Figure 9

Figure 10

19

Figure 11

Figure 12

$B = B_p \cos^8 \theta$

40